PREDICTION OF FREE TURBULENT FLOWS

BY

A. K. RASTOGI

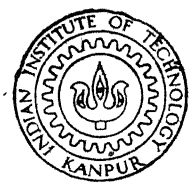

DEPARTMENT OF MECHANICAL ENGINEERING

INDIAN INSTITUTE OF TECHNOLOGY KANPUR

August, 1969

PREDICTION OF FREE TURBULENT FLOWS.

A Thesis Submitted

In Partial Fulfilment of the Requirements

for the degree of

Master of Technology

by

Ashok Kumar Rastogi

to

Department of Mechanical Engineering

INDIAN INSTITUTE OF TECHNOLOGY, KANPUR
INDIA

AUGUST
1969

C E R T I F I C A T E

This is to certify that this work has been carried out under my supervision and has not been submitted elsewhere for a degree.

Dr. S.V. [illegible]
Assistant Professor
Dept. of Mech. Engg.
I.I.T./K A N P U R.

LIST OF CONTENTS

3. Results and discussions.

(3.1) The plane mixing layer.

(3.2) The plane jet.

(3.3) The round axisymmetric jet.

(3.4) The fan jet.

(3.5) General remarks.

(3.6) Effect of free-stream turbulence.

References.

Nomenclature.

Appendix.

A_B_S_T_R_A_C_T

Free turbulent flows are predicted using an implicit, finite difference procedure for solving the boundary layer equations. Prandtl mixing length theory, Kolmogorov - Prandtl model and Kolmogorov - Prandtl -Rotta model of turbulence are used for finding the expression of effective viscosity. It is shown that Kolmogorov-Prandtl - Rotta model of turbulence predicts all the free flows satisfactorily using only one set of empirical constants unlike the Prandtl mixing length theory and Kolmogorov - Prandtl model. The question why different empirical constants are needed for mixing length theory to predict the different free flows is answered with the help of Rotta's length scale used in Kolmogorov - Prandtl - Rotta model of turbulence.

ACKNOWLEDGEMENTS

The author expresses his deep sense of gratitute and indebtedness to Professor Suhas Vasant Patankar for his invaluable guidance and constant encouragement throughout this work. He would also like to thank Professor Vasant Ram for kindly translating Rotta's paper without which this work would not have been possible.

INTRODUCTION

(0.1) Motivation for studying free turbulent flows :-

The study of free turbulent flows, such as a high-velocity jet issuing from a thin slot or from a round opening into stagnant surroundings, forms the preliminary stage in the study of turbulent boundary layers. In these flows, due to the absence of wall, we can completely ignore the viscosity effects thus introducing considerable simplification. Even in the turbulent boundary layers along ~~the~~ walls, about 70% of the boundary layer thickness near the outer edge has little effect of viscosity and so the study of free flows helps to a great extent in understanding the turbulent boundary layers on walls. Apart from this, free flows have many practical applications, some of which are mentioned below :-

(1) In the combustion chamber of a gas-turbine engine, the air necessary for combustion and for cooling is introduced in the form of jets. Jet calculations are useful in the design of such combustion chambers.

(2) Use of jets in the form of air-curtains for protecting the room from cold or hot winds is very effective.

(3) Two-phase jets, consisting of a mixture of a gas with solid particles or liquid droplets, are encountered in the combustion chambers of jet - engines and industrial furnaces, atomizing paint sprays, sand blasting equipment etc.

(4) Jet calculations play a very important role in the design of modern open-jet wind tunnels.

(5) Now it is commonly believed that the mechanism of generation of aerodynamic sound in jets depends highly upon the intensity of turbulence in the initial part of the jet. Thus the study

of turbulence - intensity in jets becomes a practically important question.

(6) Hunter Rouse in 1953 has connected the phenomenon of cavitation with that of jet diffusion since the former occurs under certain conditions at the cores of turbulent eddies. This happening depends upon velocity and pressure fluctuations and is statistical in nature.

(7) Jets impinging on surfaces are used for drying a surface in textile and paper industries.

(0.2) <u>The problem considered</u> :-

Figure -1 shows the four types of free turbulent flows we shall deal with.

Fig.(1-a) shows a high velocity stream mixing with stagnant surroundings over the edge of a corner. The region of high velocity gradient grows in the form of a wedge and is called a plane mixing layer.

Fig.(1-b) shows a jet issuing out from a thin slot. When the surrounding velocity is zero or small, there will develop two plane mixing layers at the two edges of the slot. These two mixing layers will join at some point downstream of the slot opening and will give rise to a velocity-profile in the main region of the jet as shown in the figure. The shaded part in the mixing zone of the jet is called the potential core, as the flow in this region obeys potential-flow relations. The region between the main jet and mixing zone is called the transition zone.

Fig. (1-c) shows a jet coming out of a round opening. Here we have an axis of symmetry which coincides with the centre line of the jet. This round axisymmetric jet also is divided into three zones similar to a plane jet.

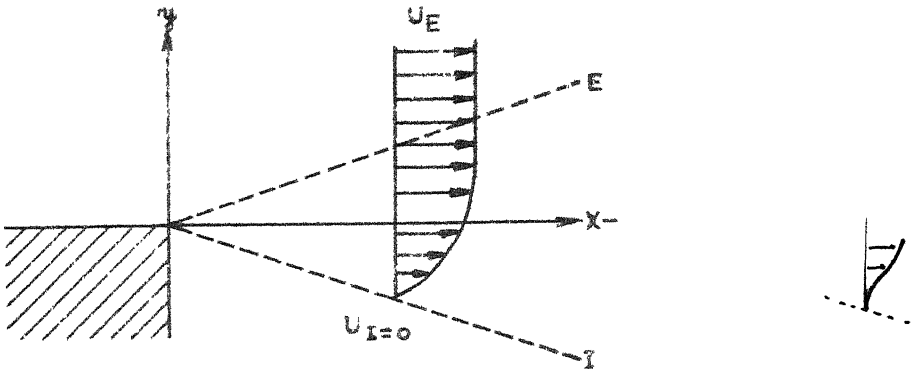

FIG. (1-a) THE PLANE MIXING LAYER

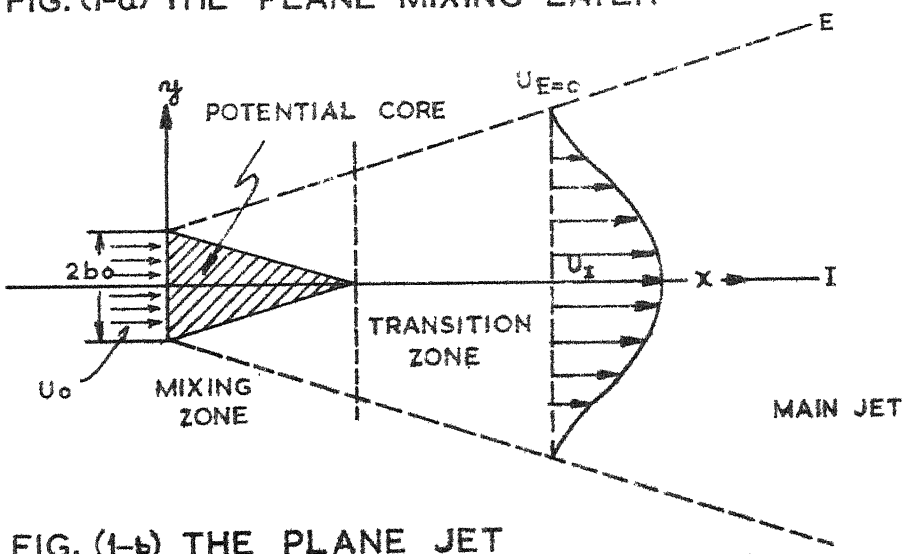

FIG. (1-b) THE PLANE JET

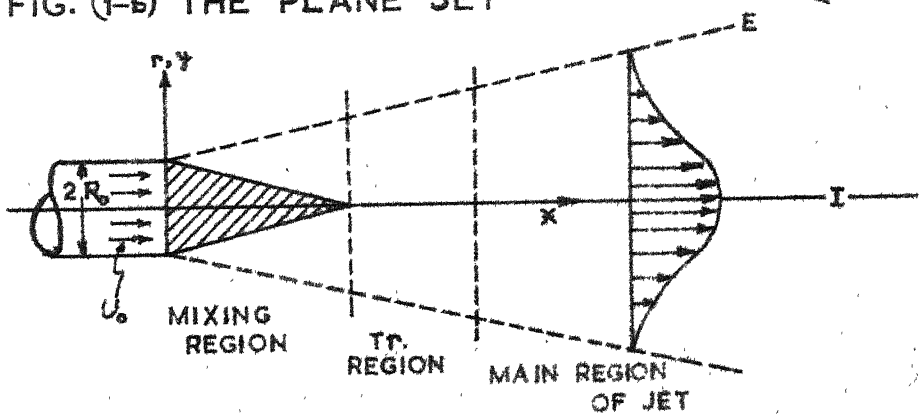

FIG. (1-c) THE ROUND AXISYMMETRIC JET

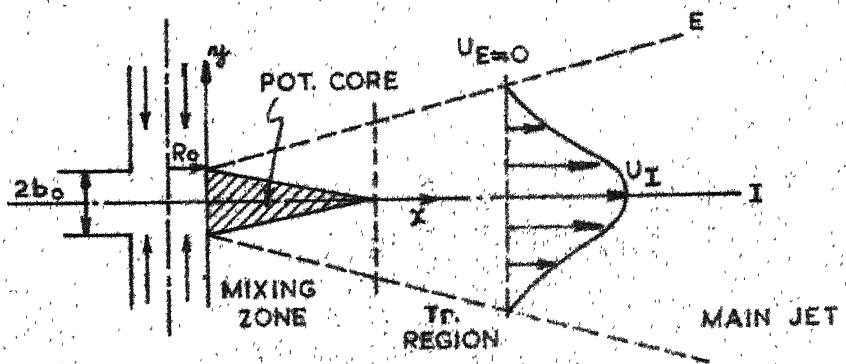

FIG. (1-d) THE FAN JET

Fig. (1-d) shows a fan jet which comparatively is not so familiar. A thin slit is cut along the periphery of a round pipe and fluid comes radially outwards through it. Here the axis of symmetry and the centre line of the jet are at right angles. The three zones have been shown in the figure. In all the four cases we will restrict ourselves to stagnant surroundings for convenience; but this restriction can be easily removed and is not essential.

It has been experimentally found out that plane mixing layer, plane jet, fan jet and also the round jet grow at nearly the same rate and have similar velocity profiles. These similarities between them should be explained by the theory used in prediction of these flows. The theories developed so far for turbulent boundary layers use the expressions for the effective viscosity that contain some empirical constants. Surprisingly enough the empirical constants necessary for each of these flows are different.

Ideally we should be able to predict all of these flows equally well, using the same empirical information in the prediction procedure. With this aim we shall predict these flows using different theories of turbulence and try to establish a set of universal constants.

(0.3) Outline of the thesis :-

Firstly we use the Prandtl (1925) mixing-length hypothesis that characterises the local state of turbulence by a local mean-velocity gradient and a local length scale. This length scale is usually taken as proportional to the width of the boundary layer, and the constant of proportionality is chosen such that the agreement between theory and experiment is satisfactory.

The evaluation of a different constant for each type of flow is demonstrated in this thesis mainly to see the suitability of the solution procedure used.

Secondly we use the hypothesis given by Kolmogorov (1942) and Prandtl (1945), referred to as K-P model hereafter, which characterises the state of turbulence by the kinetic energy of the fluctuating motion and a length scale that is again proportional to the width of the boundary layer. This model of turbulence, as shown in section (1.32), involves some more empirical constants which have to be given a different value for each flow situation.

Lastly we use an extension of K-P model which is known as Kolmogorov - Prandtl - Rotta model of turbulence and is referred to as K-P-R model. Spalding [Ref.10] has indicated that a universal set of constants can be found if K-P model is used along with the differential equation for the length scale given by Rotta (1951). By using this model the possibility of getting a universal set of constants has been explored in this thesis.

The structure of the thesis has been divided in three chapters. The first chapter gives the mathematical formulation of the problem. Section (1.1) gives the coordinate system used, and the next section (1.2) derives the conservation equation for momentum. The main features of K-P model and K-P-R model of turbulence are given in section (1.3). Boundary conditions given in section (1.4) make the problem mathematically solvable.

The second chapter of the thesis briefly describes the solution procedure. Here the finite - difference procedure developed by Patankar and Spalding (1967) is used. The material present in this chapter is repetition from [Ref.6] and is given

here for the sake of completeness.

The last chapter of the thesis is devoted to results, discussion and conclusions. Predictions are compared with the exact solutions and the experimental results.

Appendix contains some details of the derivations of different conservation equations given in section (1.3) of chapter-1.

CHAPTER-1

Mathematical formulation of the problem :-

We will treat the flows under consideration as the boundary-layer type of flows because the experimental evidence for these flows shows one predominant direction of flow and high gradients of velocity and other dependent variables perpendicular to the direction of flow. We will apply the boundary-layer approximations to general elliptic conservation equations to get the boundary-layer equations which are parabolic in nature. Absence of reverse flow is an implicit rectriction on boundary-layer approximations and therefore reverse flow should not be present in our flows. We will consider only two-dimensional flows. For the sake of convenience, we will not consider the effect of pressure gradient, compressibility, body-forces, chemical reaction etc.

(1.1) Coordinate - system :-

We choose two-dimensional axisymmetric coordinate system which meets the requirements of the present flows best. As shown in Fig.-1 the whole region of interest is considered to lie between two imaginary boundaries I (the internal boundary) and E (the external boundary). x and y are the streamwise and the cross-stream coordinates respectively. I boundary coincides with the line of symmetry in the plane jet and with the axis of symmetry in case of round jet. ~~and fan jet.~~ It should be noted that in round jet radius at any point is equal to the y coordinate at that point while in the fan jet radius increases in the direction of x and is given by $r = R_o + x$.

(1.2) Equation of conservation for momentum :-

Firstly, we shall derive the equation in the more

familiar cartesian coordinate system and then transform it to the axisymmetric coordinate system. We will use x_i $(i=1,2,3)$ for cartesian coordinate axes and u_i $(i=1,2,3)$ for the cooresponding instantaneous values of velocities. The general continuty and Navier - Stokes equations of motion for steady, incompressible fluid flow have the following form:

$$\frac{\partial u_1}{\partial x_1} + \frac{\partial u_2}{\partial x_2} + \frac{\partial u_3}{\partial x_3} = 0 \qquad (1)$$

$$u_j \frac{\partial u_i}{\partial x_j} = -\frac{1}{\rho}\frac{\partial p}{\partial x_i} + \nu \nabla^2 u_i \qquad (2)$$

After applying the boundary layer approximations to eq. (2) we get the following equation for two dimensional boundary layer flows :

$$u_1 \frac{\partial u_1}{\partial x_1} + u_2 \frac{\partial u_1}{\partial x_2} = \nu \frac{\partial^2 u_1}{\partial x_2^2} - \frac{1}{\rho}\frac{\partial p}{\partial x_1} \qquad (3)$$

Now decomposing the velocities in a time-averaged component $\overline{u_i}$ and a fluctuating component u_i' in eq. (3) and then taking the time average of the complete equation we obtain

$$\rho \overline{u_1} \frac{\partial \overline{u_1}}{\partial x_1} + \rho \overline{u_2} \frac{\partial \overline{u_1}}{\partial x_2} + \rho \frac{\partial \overline{u_1^2}}{\partial x_1} = \mu \frac{\partial^2 \overline{u_1}}{\partial x_2^2} - \rho \frac{\partial}{\partial x_2}(\overline{u_1' u_2'}) - \frac{\partial \overline{p}}{\partial x_1} \qquad (4)$$

where $\overline{p}$ is the time-averaged pressure. The first two terms of eq. (4) represent convection of momentum and the third term is generally negligible. The first term on the right hand side of eq. (4) represents the molecular diffusion of momentum due to viscous shear stresses and is negligible for our purposes. The second term represents the turbulent diffusion of momentum due to Reynold stresses $\rho \overline{u_1' u_2'}$. Last term of eq. (4) is also zero for our flows. Removing the negligible terms and transforming to

axisymmetric coordinate system we get the required conservation equation for momentum as :

$$\rho \bar{u}_1 \frac{\partial \bar{u}_1}{\partial x_1} + \rho \bar{u}_2 \frac{\partial \bar{u}_1}{\partial y} = -\frac{1}{r} \frac{\partial}{\partial y} \left(r \rho \overline{u_1' u_2'} \right) \qquad (5)$$

(1.3) Expression for effective viscosity :-

To make the mathematical solution convenient, it is customary in turbulent-flow analysis to describe the exchange laws analogous to those for laminar flows. For momentum the exchange law can be written as

$$-\rho \overline{u_1' u_2'} = \mu_{eff} \cdot \frac{\partial u_1}{\partial y} \qquad (6)$$

where μ_{eff} is the effective exchange coefficient and is called the effective viscosity.

This section deals with the three different physical hypotheses employed in the present work to express the effective viscosity in terms of known flow parameters.

(1.31) Prandtl mixing-length theory :-

Prandtl gave this theory in 1925 and is the first theory that has been widely used and has given predictions which are in good agreement with experimental results. According to this theory, the effective viscosity is given by the following relation:

$$\mu_{eff} = \rho l^2 \left| \frac{\partial \bar{u}_1}{\partial y} \right| \qquad (7)$$

where $l = \lambda y_L$

In eq. (7) l is known as Prandtl's mixing length. y_L is some characteristic thickness of boundary layer, determination of which will be given in a later chapter. λ is an empirical constant and is chosen such that predicted results agree with the

experimental ones.

The above expression for the effective viscosity along with eq. (6) completes the information required for solving eq. (5)

(1.32) Kolmogorov - Prandtl model of turbulence :-

Unlike the Prandtl mixing-length theory, K-P model characterises the state of turbulence by the kinetic energy of fluctuating motion k and a length scale L . This length scale is again taken as proportional to some characteristic thickness of boundary layer but may be different from Prandtl's mixing length l . Hence we can write that

$$\mu_{eff} = \mu_{eff}\,\{\rho, k, L\} ,$$

which leads to the following relation after dimensional analysis:

$$\mu_{eff} = C_\mu \rho k^{1/2} L , \qquad (8)$$

where C_μ = an empirical constant

and $L = \lambda_1 y_L$. λ_1 can be combined with C_μ so that we need only one empirical constant. This results in the following relation :

$$\mu_{eff} = \rho k^{1/2} L \qquad (9)$$

where $L = \lambda_{k\text{-}\rho} \cdot y_L$ $(\lambda_{k\text{-}\rho} = \lambda_1 C_\mu)$.

Physically this theory seems more realistic as it gives the effective shear stress coefficient in terms of fluctuating kinetic energy. When there are no fluctuations , $k = 0$ and hence $\mu_{eff} = 0$ which should be so.

Now when we substitute eq. (9) with eq. (6) in momentum equation (5), the latter gets coupled with k and so before we can solve the momentum equation we should have the conservation equation for k . Equation of conservation for k $\left(= \sum_{i=1}^{3} \frac{1}{2} \overline{u_i'^2}\right)$ is derived in the following way:

Step I:

We time-average each equation given by eq. (2) and

multiply each of them by the corresponding $\bar{u}_i$. By adding the three equations then, we get the equation for kinetic energy of mean motion.

Step II:

We time average each equation of eq. (2) after multiplying by the corresponding u_i . Addition of the resulting equations gives the equation for mean of total kinetic energy.

Step III:

Subracting the equation obtained in step I from the equation obtained in Step II we get the general equation for k . Then we apply boundary layer approximations to this general equation and get the required equation for k which can be written in the following form in cartesian coordinates

$$\rho \bar{u}_1 \frac{\partial k}{\partial x_1} + \rho \bar{u}_2 \frac{\partial k}{\partial x_2} = \rho \nu \frac{\partial^2 k}{\partial x_2^2} - \rho \overline{u_1' u_2'} \frac{\partial \bar{u}_1}{\partial x_2} - D - \rho \frac{\partial}{\partial x_2} \left(\overline{\frac{u_1'^2 u_2'}{2} + \frac{u_2'^2 u_2'}{2} + \frac{u_3'^2 u_2'}{2}} \right) \tag{10}$$

where

$$D = \rho \nu \left[2 \overline{\left(\frac{\partial u_i'}{\partial x_i} \right)^2} + \overline{\left(\frac{\partial u_1'}{\partial x_2} + \frac{\partial u_2'}{\partial x_1} \right)^2} + \overline{\left(\frac{\partial u_1'}{\partial x_3} + \frac{\partial u_3'}{\partial x_1} \right)^2} + \overline{\left(\frac{\partial u_2'}{\partial x_3} + \frac{\partial u_3'}{\partial x_2} \right)^2} \right]$$

The algebra involved in reaching eq. (10) can be seen in [Ref.7] . The left hand side of eq. (10) represents convection of k by the mean motion. The first term on right hand side represents molecular diffusion of k and is negligible for our flows. The second term represents interaction between turbulent stresses and mean velocity gradient. Turbulent stresses tend to create k from the mean motion and thus this term represents generation of k . D in eq. (10) represents the effect of laminar viscosity on fluctuating motion. In fact this is the effect of fluctuating laminar stresses on velocity fluctuations which means dissipation of turbulence. The last term of eq. (10) represents the transport

of k by fluctuations themselves which is turbulent diffusion of k. This way eq. (10) shows that at a pt. in turbulent flow kinetic energy of fluctuating motion is convected, diffused, produced and dissipated. The dissipation and generation terms are combined together and are called the source term. Writing eq. (10) in our axisymmetric coordinate system we have

$$\rho \bar{u}_1 \frac{\partial k}{\partial x} + \rho \bar{u}_2 \frac{\partial k}{\partial y} = -\frac{1}{r} \frac{\partial}{\partial y} (r J_k) + \Phi_k \qquad (11)$$

where Φ_k = source term

$$= \left[-\rho \overline{u_1' u_2'} \frac{\partial \bar{u}_1}{\partial y} - D \right]$$

and J_k = turbulent diffusional flux of k in the cross - stream direction and has the following form

$$= \left[\frac{\overline{u_1'^2 u_2'}}{2} + \frac{\overline{u_2'^2 u_2'}}{2} + \frac{\overline{u_3'^2 u_2'}}{2} \right]$$

J_k is analogous to ~~negative of~~ Reynold stresses in the momentum equation and is to be expressed by an exchange law similar to eq. (6). The exchange law for k is defined as

$$J_k = -\Gamma_{k,eff} \frac{\partial k}{\partial y} \qquad (12)$$

where $\Gamma_{k,eff}$ is the effective exchange coefficient. Following the definition of laminar Prandtl number, we define the effective Prandtl no. for k as

$$\sigma_{k,eff} = \mu_{eff} / \Gamma_{k,eff} \qquad (13)$$

The expression of D as given by eq. (10) contains the fluid viscosity which may imply that dissipation of k occurs due to viscous effects, but as explained by Emmons [Ref.3] the dissipation of turbulent energy is controlled by energy transfer process rather than the viscous effects. The velocity fluctuations can be visualised as eddies of different sizes. Larger eddies have more kinetic energy and kinetic energy is transferred from larger

eddies to smaller eddies till eddies become so distorted that the fluctuating energy is dissipated as heat by viscosity. Therefore dissipation should be a function of k and the length scale L. From the expression of D in eq. (10) we can write

$$D = D\{\rho, k, L\}$$

Dimensional analysis leads to

$$D = C_D \rho k^{3/2}/L \qquad (14)$$

C_D in eq. (14) is again an empirical constant. Eq. (14) is in accordance with the energy transfer process as D is larger for larger k_s'. This completes the K-P model of turbulence which requires simultaneous solution of eq. (5) and eq. (11).

(1.33) <u>Kolmogorov - Prandtl - Rotta model of turbulence</u> :-

Effective viscosity in this model also is given by eq. (9), but L is evaluated in a different way. Rotta (1951) has given differential equations for conservation of L and (kL). He derived these equations from the general Navier Stokes equations of motion considering the statistical behaviour of turbulence. We have used the equation for (kL) in the present thesis. This equation has the following form :

$$\rho \bar{u}_1 \frac{\partial (kL)}{\partial x} + \rho \bar{u}_2 \frac{\partial (kL)}{\partial y} = \frac{1}{r} \frac{\partial}{\partial y} \left[\frac{r \mu_{eff} \sigma_Q}{\sigma_{k,eff}} \frac{\partial}{\partial y} (kL) \right] + \mu_{eff} L \sigma_{12} \left(\frac{\partial \bar{u}_1}{\partial y} \right)^2 - D L \sigma_s , \qquad (15)$$

where σ_Q, σ_{12}, σ_s are empirical constants. This equation is very similar to previous equations for momentum and k. The left hand side is the convection of (kL) while the right hand side terms represent diffusion, generation and dissipation of (kL). Derivation of eq. (15) is given in the appendix. With eq. (15) we have three parabolic partial differential equations to be solved

simultaneously while using K-P-R model of turbulence.

(1.4) Boundary conditions :-

Boundary conditions to the equations to be solved will depend upon the nature of I and E boundaries. We can have the following two types of boundaries:

(i) Free - boundary: It refers to the situation when the boundary is adjacent to an inviscid free stream such as both the edges of a mixing layer or the outer boundary of a jet. Value of the dependent variable namely the longitudinal velocity $\bar{u}_1$ or fluctuating kinetic energy k or (kL), at the free boundary should be equal to the of the free stream.

(ii) Symmetry - line boundary: When a boundary coincides with the line of symmetry (I boundary of a plane jet) or the axis of symmetry (I boundary of a round jet), it is known as symmetry-line boundary. The value of the dependent variable along this line is unknown while the gradients normal to this line are zero.

CHAPTER - 2

Method of solution :-

We will not go into the comparative study of different methods of solution. It has been well known now that finite difference methods work as well as any other method if used with an economical computation procedure.

(2.1) Choice of coordinates:-

Purpose of this section is the judicious selection of coordinates in stream-wise and cross-stream directions. Efficiency of finite difference methods depends largely upon the coordinate system being used. Since the boundary layer grows in thickness with downstream distance, the grid used should adjust itself to conform with the boundary layer thickness. Also the cross-stream variable should be monotonic. These requirements are fulfilled by $x \sim \omega$ coordinate system where ω is the nondimensionalised stream function defined by $\omega \equiv \frac{\psi - \psi_I}{\psi_E - \psi_I}$. This definition is such that $\omega = 0$ at I boundary and $\omega = 1$ at the E boundary. From the definition of stream function we have

$$\left.\begin{aligned} \frac{d\psi_I}{dx} &= -\rho_I \dot{m}''_I \\ \frac{d\psi_E}{dx} &= -\rho_E \dot{m}''_E \end{aligned}\right\} \qquad (16)$$

where $\dot{m}''_I$ and $\dot{m}''_E$ are the rates of mass transfer across I & E boundaries respectively. These are called the entrainment rates and how to obtain these is an important problem which will be solved later in this chapter.

Transforming the conservation equations derived in chapter 1

to $x \sim \omega$ coordinates we can write them in the following form :

Conservation of momentum:

$$\frac{\partial \bar{u}_1}{\partial x} + \frac{\{(1-\omega)r_I \dot{m}_I'' + \omega r_E \dot{m}_E''\}}{(\psi_E - \psi_I)} \frac{\partial \bar{u}_1}{\partial \omega} = \frac{\partial}{\partial \omega}\left\{ \frac{r^2 \rho \bar{u}_1 \mu_{eff}}{(\psi_E - \psi_I)^2} \frac{\partial \bar{u}_1}{\partial \omega} \right\} \qquad (17)$$

Conservation of k :

$$\frac{\partial k}{\partial x} + \frac{\{(1-\omega)r_I \dot{m}_I'' + \omega r_E \dot{m}_E''\}}{(\psi_E - \psi_I)} \frac{\partial k}{\partial \omega} = \frac{\partial}{\partial \omega}\left\{ \frac{r^2 \rho \bar{u}_1 \mu_{eff}}{(\psi_E - \psi_I)^2 \sigma_{k,eff}} \frac{\partial k}{\partial \omega} \right\} + \frac{1}{\rho \bar{u}_1}\left[\mu_{eff} \frac{\rho^2 r^2 \bar{u}_1^2}{(\psi_E - \psi_I)^2} \left(\frac{\partial \bar{u}_1}{\partial \omega}\right)^2 - C_D \rho k^{3/2}/L \right] \qquad (18)$$

Conservation of (kL) :

$$\frac{\partial (kL)}{\partial x} + \frac{\{(1-\omega)r_I \dot{m}_I'' + \omega r_E \dot{m}_E''\}}{(\psi_E - \psi_I)} \frac{\partial}{\partial \omega}(kL) = \frac{\partial}{\partial \omega}\left\{ \frac{r^2 \rho \bar{u}_1 \mu_{eff}}{(\psi_E - \psi_I)^2 \sigma_{kL,eff}} \frac{\partial}{\partial \omega}(kL) \right\} + \frac{1}{\rho \bar{u}_1}\left[\mu_{eff} \frac{\rho^2 \bar{u}_1^2 r_L^2}{(\psi_E - \psi_I)^2} f_{12} \left(\frac{\partial \bar{u}_1}{\partial \omega}\right)^2 - f_s C_D k^{3/2} \rho \right] \qquad (19)$$

where $\sigma_{kL,eff} = \sigma_{k,eff}/f_Q$

Simplifying the appearance of the above equations they can be put in the following common form :

$$\frac{\partial \phi}{\partial x} + (a + b\omega)\frac{\partial \phi}{\partial \omega} = \frac{\partial}{\partial \omega}\left(c \frac{\partial \phi}{\partial \omega}\right) + d \,, \qquad (20)$$

where ϕ stands for the dependent variable and

$$a \equiv r_I \dot{m}_I'' / (\psi_E - \psi_I)$$

$$b \equiv (r_E \dot{m}_E'' - r_I \dot{m}_I'') / (\psi_E - \psi_I)$$

$$c \equiv (r^2 \rho \bar{u}_1 \mu_{eff}) / (\psi_E - \psi_I)^2 \sigma_{eff}$$

$d \equiv 0$ for momentum

$$\equiv \frac{\mu_{eff} r^2 \rho \bar{u}_1}{(\psi_E - \psi_I)^2}\left(\frac{\partial \bar{u}_1}{\partial \omega}\right)^2 - \frac{C_D k^{3/2}}{L \bar{u}_1} \quad \text{for } k$$

$$\equiv \frac{\mu_{eff} r^2 \rho \bar{u}_1 L}{(\psi_E - \psi_I)^2} f_{12}\left(\frac{\partial \bar{u}_1}{\partial \omega}\right)^2 - f_s C_D k^{3/2}/\bar{u}_1 \quad \text{for } (kL)$$

(2.2) Finite difference equations :-

The standard finite-difference procedure is to divide the field of interest by a number of grid lines drawn in streamwise as well as cross-stream directions. The dependent variables at the neighbouring nodes are related to each other through difference equations. The equation is to be solved by marching-integration procedure. $\phi \sim \omega$ profile will be known at a value of x and will be required at a greater value of x . The problem of obtaining these difference equations from the general partial differential equation (20) is briefly described in this section.

The usual method of obtaining a finite difference equation from a partial differential equation is to make use of Taylor-series expansion. However, a different procedure has been used here; the difference equation is obtained by expressing each term in the parent partial differential equation as an integrated average over a miniature control volume. This can be explained by the following sketch:-

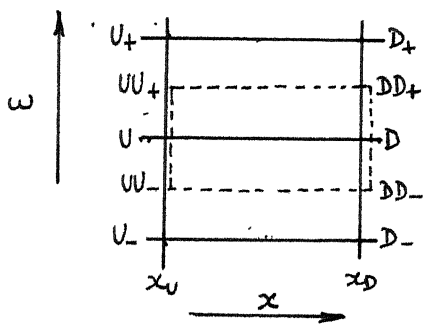

The sketch shows a portion of the grid. The points U and D are upstream and downstream nodes respectively at a given ω value. $U+$ and $U-$ are the points at the nearby ω values at upstream station and $UU+$ is a point midway between U and $U+$ while $UU-$ is a point midway between U and $U-$. Similar nomenclature is used at downstream station. The broken line shows the control volume. If we consider the nodal point D, we shall express each term of eq.(20) as an integrated average over this control volume. Evaluation of

the integrals involved requires the variation of ϕ between the grid points. We shall assume that ϕ varies linearly with ω and has a stepwise variation with respect to x having the downstream value throughout the interval except at x_U . Also partial derivatives with respect to ω are evaluated at the downstream station. This practice is followed as it is free from the problem of instability for large step lengths and is more convenient. If we evaluate the $\partial/\partial\omega$ terms at the upstream station, the method would correspond to the explicit Dufort-Schmidt method which is unstable for large step lengths. The method, which corresponds to Crank & Nicholson's procedure, is to have the arithmetic mean of the values of $\partial/\partial\omega$ terms at x_U and x_D .

Following these general rules we get the following difference equation for the nodal point D :

$$\phi_D = A\,\phi_{D_+} + B\,\phi_{D_-} + C \qquad (21)$$

where A, B and C are known coefficients and contain the values of a, b and c evaluated at the upstream station x_U . Such finite difference equations are found for all the grid points at x_D ranging from $\omega = 0$ to $\omega = 1$ and are solved simultaneously to give profile at x_D .

(2.3) Miscellaneous matters :

(2.31) Calculation of entrainment rates:-

The coefficients A, B and C of the difference equation (21) contain a, b and c evaluated at the upstream station. Thus evaluation of a, b and c becomes necessary before coming to solve the difference equations. Also a & b as given in eq. (20) give us the entrainment rates that control the boundary layer growth. The present section deals with the evaluation of these entrainment rates.

Main thing to consider is that the I and E boundaries which

are arbitrary should be so chosen that they enclose the whole region of interest. When the boundary layer encloses a symmetry line, the choice is straight forward. It is most convenient to coincide one of the boundaries with the symmetry line. Since there is no flow across a symmetry line 'a' will be zero if I boundary coincides with the symmetry line and $(a+b)$ will be zero if E boundary coincides with the symmetry line.

In case of free boundaries the choice of I and E edges becomes less obvious. Here it depends upon the effective viscosity law whether the edge can be specified without arbitrariness or not. We will consider two cases:

(I) When the effective viscosity vanishes at the boundary as in Prandtl mixing length theory. Application of this theory results in a definite thickness of the boundary layer.

(II) When μ_{eff} does not vanish at the boundary such as in K-P model or K-P-R model. In such cases the edge is arbitrary and approach to free-stream conditions is asymptotic.

Case (I) : We write the eq. (20) at $\omega=\omega_D$ near E - boundary in the following form:

$$(a+b\,\omega_D) = \left[\frac{\frac{\partial}{\partial\omega}\left(c\frac{\partial\phi}{\partial\omega}\right)}{(\partial\phi/\partial\omega)}\right]_D + \frac{d_D - [\partial\phi/\partial x]_D}{(\partial\phi/\partial\omega)_D} \qquad (22)$$

Now according to Prandtl mixing length theory $\mu_{eff}=0$ at $\omega=1$, therefore we have a definite line that exactly divides a region of nonzero $(\partial\phi/\partial\omega)$ from the region of $\partial\phi/\partial\omega=0$. Thus in eq. (22) we make ω_D approach unity so that D and E surfaces become identical.

In the free stream just outside the E boundary from eq.(20) we can write $d_E = [\partial\phi/\partial x]_E$ but since D and E are identical we can write $d_D = [\partial\phi/\partial x]_D$ (23)

Changing over to physical coordinate y and putting the expression for l_{eff} from eq. (7) we have for $\phi = \bar{u}_1$

$$\left[\frac{\frac{\partial}{\partial\omega}\left(c\frac{\partial\phi}{\partial\omega}\right)}{(\partial\phi/\partial\omega)}\right]_D = \frac{2}{(\psi_E-\psi_I)}\left[r\rho\ell^2\left|\frac{\partial^2\bar{u}_1}{\partial y^2}\right|\right]_D \qquad (24)$$

Approaching $\omega=1$ from inside the boundary layer and using eq. (23) we obtain

$$(a+b) = \frac{2}{(\psi_E-\psi_I)}\left[\rho r\ell^2\left|\frac{\partial^2\bar{u}_1}{\partial y^2}\right|\right]_E \qquad (25)$$

similarly for I boundary we will put $\omega=0$ and obtain

$$a = \frac{2}{(\psi_E-\psi_I)}\left[r\rho\ell^2\left|\frac{\partial^2\bar{u}_1}{\partial y^2}\right|\right]_I \qquad (26)$$

in which again we have to approach $\omega=0$ from higher values of ω. Using the finite-difference expression for the second-order derivatives appearing above we have the following expressions for entrainments :

$$\left.\begin{aligned} \dot{m}''_I &= 8\rho_I\ell_I^2\,\frac{|u_2+u_3-2u_1|}{(y_2+y_3-2y_1)^2} \\ \dot{m}''_E &= -8\rho_E\ell_E^2\,\frac{|u_{N+1}+u_{N+2}-2u_{N+3}|}{(y_{N+1}+y_{N+2}-2y_{N+3})^2} \end{aligned}\right\} \qquad (27)$$

In eq. (27), u stands for streamwise velocity $\bar{u}_1$ and suffixes denote the grid points.

Case-II : When l_{eff} does not vanish along a definite line, we have to choose our E-boundary such that the fluid properties at E boundary do not differ too much from those at free stream. Again we use eq.(22

for $\phi = \bar{u}$ at a particular value of $\omega = \omega_D$. For $\left.\frac{\partial \bar{u}}{\partial x}\right|_D$ we use the following relation (Subscript 1 has been dropped from $\bar{u}_1$)

$$\frac{\partial \bar{u}_D}{\partial x} = \frac{\bar{u}^*_{D,d} - \bar{u}_{D,u}}{\Delta x} \tag{28}$$

where $\bar{u}^*_{D,d}$ is the desired value of velocity at the downstream station at $\omega = \omega_D$ and $\bar{u}_{D,u}$ is the value prevailing at the upstream station. The choice of $\bar{u}^*_{D,d}$ will influence the entrainment rate and thus will make the boundary layer expand or contract. With the use of eq. (28), right hand side of eq. (22) can be evaluated. Let us say that near $\omega = 1$, $\omega_D = \omega_{D_1}$ and

$$a + b\omega_{D_1} = D_1 \tag{29}$$

If I boundary is a symmetry line boundary $a = 0$ and $\dot{m}''_E$ is obtained from eq. (29). In case I boundary is also a free boundary, the same procedure is applied at that boundary. We apply eq. (22) at $\omega = \omega_{D_2}$ near I boundary and find

$$a + b\omega_{D_2} = D_2 \tag{30}$$

Solving simultaneously eq. (29) and eq. (30) we get

$$a = \frac{\omega_{D_2} D_1 - D_2 \omega_{D_1}}{\omega_{D_2} - \omega_{D_1}}$$

$$b = \frac{D_1 - D_2}{\omega_{D_1} - \omega_{D_2}} \tag{31}$$

(2.32) Calculation of cross - stream distance :-

From the $\phi \sim \omega$ profile it is essential to obtain $\phi \sim y$ profiles to get the physical idea of the solutions. Secondly in the calculation of c in eq. (20) y'_s are needed and so to proceed the forward integrations also it is necessary to have y'_s corresponding to all the grid points. From the definition of ω we write

$$\int_0^y \rho dy = (\psi_E - \psi_I) \int_0^\omega (\rho \bar{u})^{-1} d\omega \tag{32}$$

The left hand side is known in terms of y as we know the relation between r and y such as $r=y$ in case of a round axisymmetric jet. Integral appearing in the right hand side of eq. (32) can also be evaluated for two adjacent grid points by numerical methods provided ρ or $\bar{u}$ does not vanish at any grid point. Thus can be evaluated at all the grid points.

(2.33) Choice of characteristic thickness of the boundary layer :-

The physical thickness of the boundary layer from I to E boundary is calculated from $\bar{u} \sim \omega$ profile but this thickness is not used as the characteristic thickness of the layer as it is subject to arbitrariness. The characteristic thickness y_L is defined as the distance between the two points in the boundary layer, one near I boundary and the other near E boundary. This point comes on the boundary itself in case of symmetry line boundary. For free boundary this point is chosen such that the velocity at the point differs from the adjacent free stream velocity by some fraction of the maximum velocity difference across the layer. This fraction F can be 0.1 or 0.2. It is this y_L which is used to define Prandtl's mixing length in eq. (7). It is clear now that the value of λ will depend upon the value of F being used. Advantage of using this length is that it is free from arbitrariness.

(2.34) Choice of forward step :-

For forward integration the proper choice of Δx is very important because if Δx is taken very small, computation time will increase beyond desirable limits and if Δx is made larger instabilities will occur. With larger value of Δx profiles oscillate with large amplitude due to the fact that entrainments are evaluated at the upstream station.

To avoid both of these troubles it is a general working

rule that step length is made proportional to the boundary layer thickness. In some situations Δx can be defined like following as well:

$$\Delta x = \text{Const.}\ (\psi_E - \psi_I)_U \Big/ (\gamma_I \dot{m}''_I - \gamma_E \dot{m}''_E) \qquad (33)$$

where $.01 < \text{const.} < .05$

eq. (33) ensures that in the step length Δx, 1 to 5% of the total fluid present in the boundary layer is entrained.

(2.35) Initial profiles of the dependent variables :-

To start the forward integration we should know the $\phi \sim \omega$ profile at an upstream station. As mentioned earlier ω values from 0 to 1 are chosen or calculated first of all for making the grid and then linear $\phi \sim \omega$ variation is taken between the adjacent grid points. There is no hard and fast rule for choosing ω intervals however higher accuracy demands that ω values should be close to each other in the regions where $\phi \sim \omega$ profile changes slope rapidly such as near the boundary lines.

It is desirable that grid nodes should be equally spaced on the y-scale so as to have a $\phi \sim y$ profile which is physically compatible. This can be achieved through experience only as the profiles change with x. It should be mentioned here that efficiency of computation depends also upon the number N of grid points used. N=16 is recommended by Patankar and Spalding [Ref. 6] for satisfactory use.

The initial $\phi \sim \omega$ profiles are taken from experiments, empirical relations or guess work. In turbulent boundary layers downstream events are usually not very sensitive to upstream conditions and hence the specification of the initial profile becomes rather unimportant. All the same the initial profiles should correspond to real flow situation e.g. for mixing layer if $u_I = 0$

and u_E = constant we can have a linear variation of velocity from $u_I = 0$ at $y = 0$ to u_E = constant at $y = y_E$. Similarly if the turbulent energy of the surroundings of the mixing layer is zero, we can take linear variation of k with respect to y varying from zero at the boundaries to a finite value at some point near midway of the boundary layer thickness.

CHAPTER -3

Results and discussions :-

We will consider the results obtained by using all the three hypotheses of turbulence for each flow situation in a separate section. Then will follow the advantages of one hypothesis over the other.

(3.1) The plane mixing layer :-

a) Use of Prandtl mixing-length theory:-

Using the Prandtl mixing-length theory we have solved the partial differential equation for momentum. To ensure the suitability of the prediction method we have compared the solution with the exact solution of this problem given by Tollmien (1926). The excellent agreement between the velocity profile given by Tollmien (Ref.1) and that obtained by our method can be seen in fig. 2. It can be deduced from the Tollmien's solution that

$$\frac{y_L/x}{\lambda^2} = 3.94 \quad \text{for } F = .2$$

The value obtained in the present solution is 3.962. We conclude from this that our solution procedure is satisfactory. Comparison of the exact solutions with our solutions using the present theory for the other flow situations will not be reported in this thesis, since the two solutions are the same as demostrated by fig. 2.

We stop the integrations when the velocity profiles cease to change. In this equilibrium state, the boundary layer thickness grows linearly with x and rate of growth of the boundary layer is measured by y_E/x . The value of y_E/x =.266 in the present solution which compares very well with the experimental value of .27. The value of λ which is the only empirical constant needed with this theory was 0.117 with F =.1 and .16 with F =.2. The step length was increased with the growth of boundary layer and

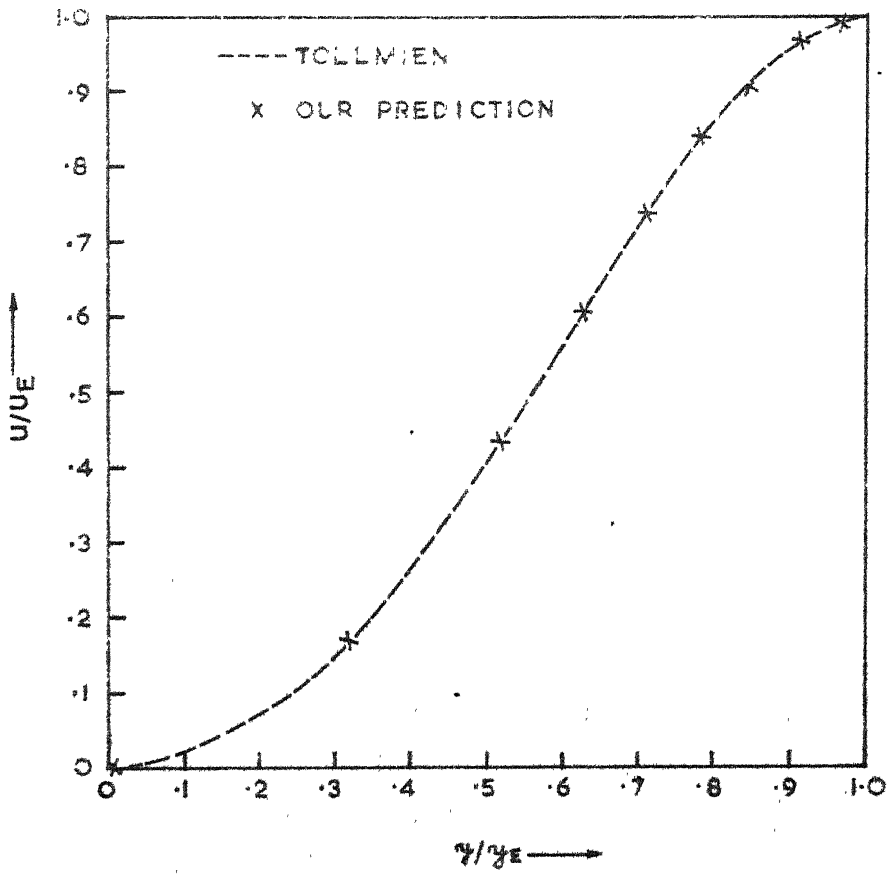

FIG. 2 DIMENSION LESS VELOCITY PROFILE IN A MIXING LAYER

largest step length used in the equilibrium region was 30% of the local boundary layer thickness.

b) Use of K-P model of turbulence:-

With the K-P model we have solved simultaneously the partial differential equations for momentum and k. The empirical constants involved are λ_{K-P}, $\sigma_{k,eff}$ and C_D that were given the following values to obtain results that agree satisfactorily with the experimental results

λ_{K-P} = .066 (with F = .1); $\sigma_{k,eff}$ = 2.5, C_D = .1

A rough estimate of these constants has been given by Glushko in 1965 and by Spalding in 1966. We started computations with their constants and reached at the above set of constants by hit and trial so that some gross quantities of the flow such as the rate of growth of the boundary layer and the peak value of k, as evaluated by our method matched with the experimental values. We obtained y_2/x = .152 where as the experimental value is .16 — Similarly the peak value of k obtained by us was 6.3% of the mean kinetic energy at the E boundary ($\frac{1}{2}u_E^2$) where as the value shown by the experiments is about 7.5% as shown in fig. (3-b). The dimensionless velocity profile has been shown in fig. (3-a) which compares satisfactorily with the experimental profile.

In the computations with this model the step length was kept proportional to the local boundary layer thickness. The largest step length used was 20% of the boundary layer thickness. Following considerations helped in getting the desired set of constants.

In the equilibrium region growth rate becomes constant and k profile (fig. 3 b) also becomes invariant like the velocity profile. In this region dissipation of k equals the generation.

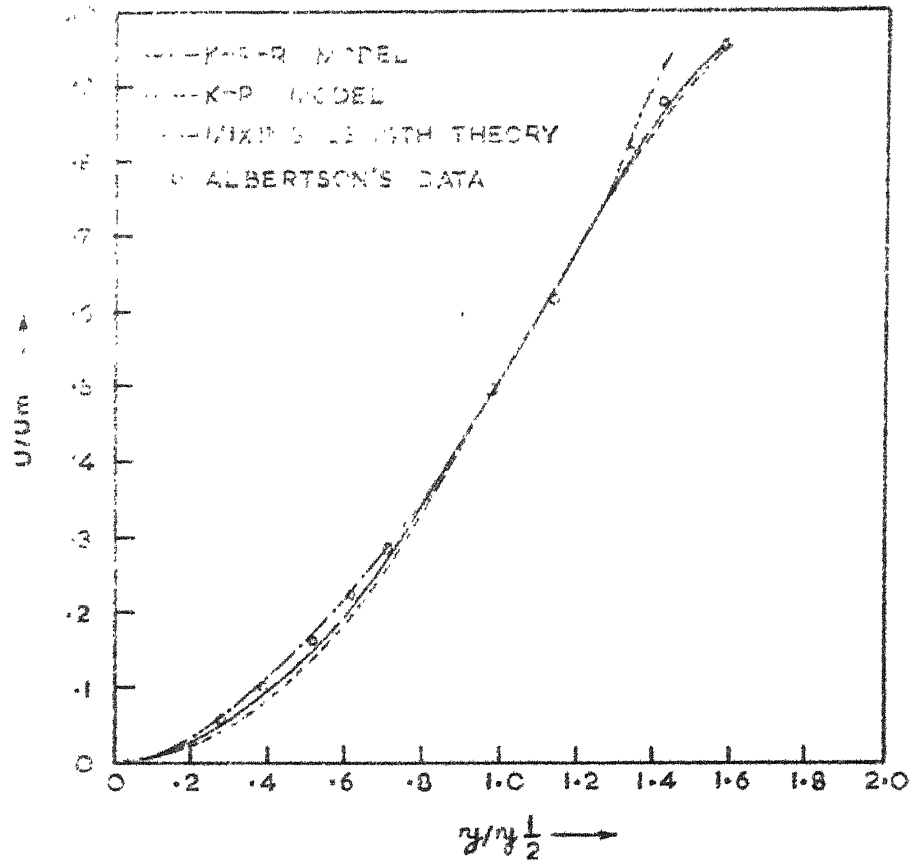

FIG.(3-a) DIMENSION LESS VELOCITY PROFILE IN A MIXING LAYER

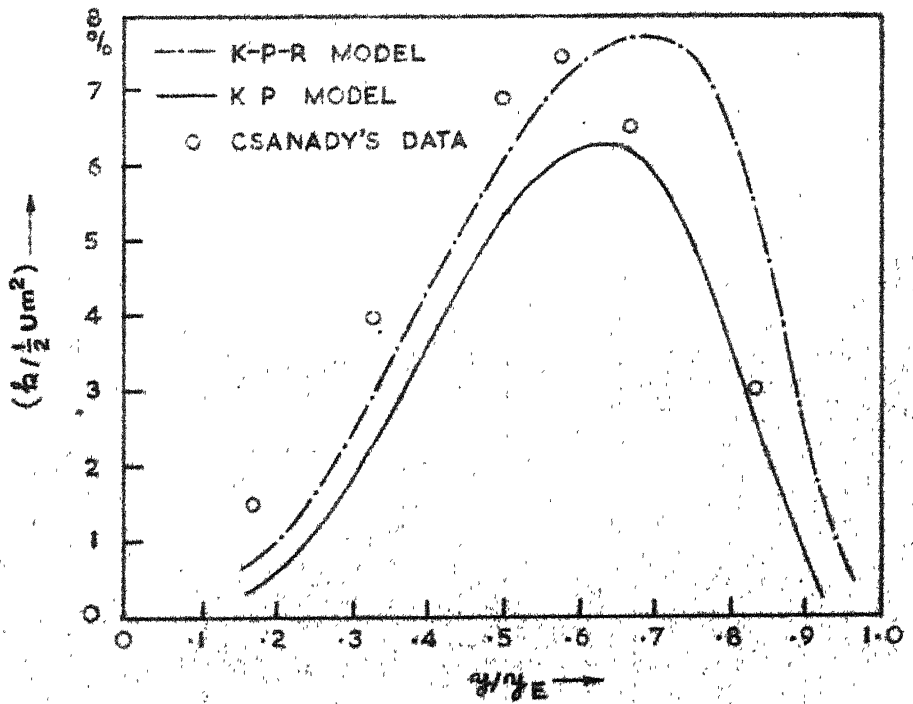

FIG. (3-b) VARIATION OF TURBULENT ENERGY k IN A MIXING LAYER

It can be shown by putting the source term of k equation equal to zero that in this region K-P model reduces to Prandtl mixing-length theory. The equivalence of the two theories is given by the relation

$$\lambda^2_{K-P} = \lambda^2 \sqrt{C_D} \qquad (34)$$

Above relation helps in finding the desired values of constants. The constant C_D appears in the dissipation term of the equation for k that contains 3/2 power of k and hence change in C_D affects the peak value of k .

c) Use of K-P-R model of turbulence :-

With the K-P-R model of turbulence the partial differential equations for momentum , k and (kL) have been solved simultaneously. The following set of constants give satisfactory results.

$C_D = .1$, $\sigma_s = .4$, $\sigma_{12} = .825$, $\sigma_{k,eff} = 2.5$; $\sigma_{kL,eff} = 2.5$

With this set of constants a value of .175 was obtained for y_L/x and peak value of k obtained was 7.8% of $(\frac{1}{2}u_E^2)$

The velocity profile as given in fig. (3-a) compares very well with the experiment profile. There is slight deviation in our predicted profile from the experimental profile near the high velocity end which is not of much significance. k profile (fig. 3-b) also is satisfactory.

It was noticed in the computations with the present model that not all the values of the constants σ_{12} and σ_s ~~do not~~ work. The reason is that in the equilibrium region the (kL) profile will not be invariant as the length scale should increase with the downstream distance. Therefore the source term of the equation for (kL) should be positive always. Since the constants σ_{12} and σ_s come in the source term of equation for (kL) , the values of these constants that make the source term negative will not give a satisfactory solution. The values of L were evaluated at some nodal

points at each station and it was seen that L increases in the proportion of corresponding y_L in the equilibrium region. Implications of this observation will be discussed lateron. The present computations become more sensitive to the size of the step length. In the initial region the step length was kept only 4% of the local boundary layer thickness while the largest step length used was 8% of the boundary layer thickness.

(3.2) The plane jet :-

The experimental results for a plane jet with which we will compare our results can be correlated by the following relations:
Rate of growth $y_{1/2}/x$ = .1 approximately
Centre line velocity u_m is given by $(u_m/u_0) = 2.5\sqrt{2b_0/x}$
which gives the potential core length = 6.25 times the slot width and the peak value of k = about 16% of

a) Use of Prandtl mixing length theory :-

The value of λ used was .1+1 for $F = .2$. To calculate the potential core length, the width of the potential core is calculated by the following relation

$$y_{pot.} = y_{pot} - \frac{\dot{m}''_I \, \Delta x}{\rho \, u_0} \qquad (35)$$

where the initial value of y_{pot} = b_0 = 1. The value of x where y_{pot} becomes zero gives the length of the potential core. With the present theory this length is about 17 where the experimental results show that it should be about 12.5 for slot width = 2. In the main region of the jet boundary-layer thickness grows linearly with x and the rate of growth is given by $y_{1/2}/x$ = .09 which is nearly equal to the experimental value.

Decay of the centre-line velocity in our solution is given by $(u_m/u_0) = 3.98/\sqrt{x}$, which is within 10% of the experimental value.

Fig. (4-b) shows the variation of the centre-line velocity with x. The velocity profile obtained in our solutions agrees very well with the experimental profile as shown in fig. (4-a).

Thus we see that the value of .141 for λ gives good agreement in the main jet region while in the mixing zone it overestimates the length of the protential core. For the mixing zone we should have a different value of λ that gives the correct length of the potential core.

b) Use of K-P model of turbulence :-

As suggested just above, to get a better agreement with experimental results in the mixing zone a different value of constant λ should be used; this practice will be adopted here. Constants used in the mixing zone are

$\lambda_{K-P} = .1$, $F = .2$, $C_D = .1$ and $\sigma_{k,eff} = 2.5$

This set of constants gives the length of the potential core equal to 13 approximately. It should be noticed here that λ_{K-P} used in mixing layer was .066 where as $\lambda_{K-P} = .1$ is used in the mixing zone of the plane jet which is nothing but a mixing layer. Higher value in the present case is expected because we are using higher value of F which decreases the value of y_L.

For the main jet region we use $\lambda_{K-P} = .108$ and keep the other constants unchanged. With this set we get the following results:

$(y_{1/2}/x) = .107$ which is within 10% of the experimental rate of growth. The centre-line velocity decays according to the following relation $(u_m/u_0) = 3.9/\sqrt{x}$ which is satisfactory. Fig. (4-b) shows some variations at lower values of x. This region belongs to transition-zone and some irregularities are expected before the centre line velocity adjusts itself according to the desired

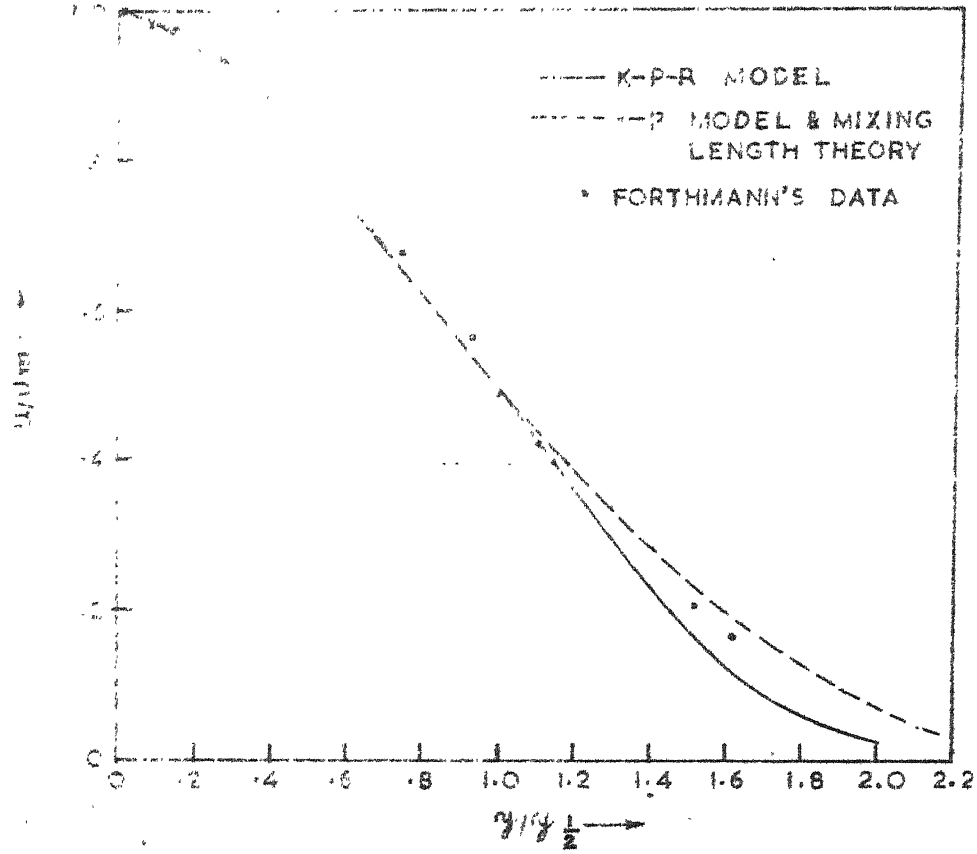

(a) DIMENSION LESS VELOCITY PROFILE

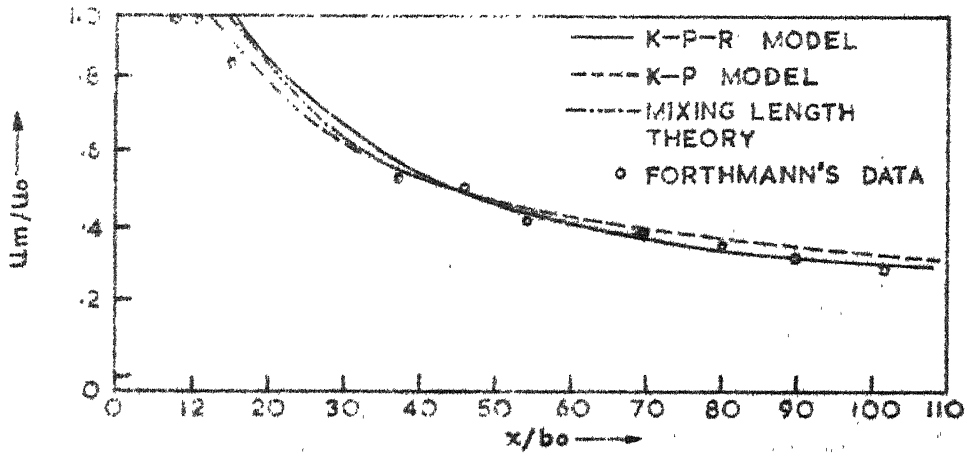

(b) DECAY OF CENTRE-LINE VELOCITY

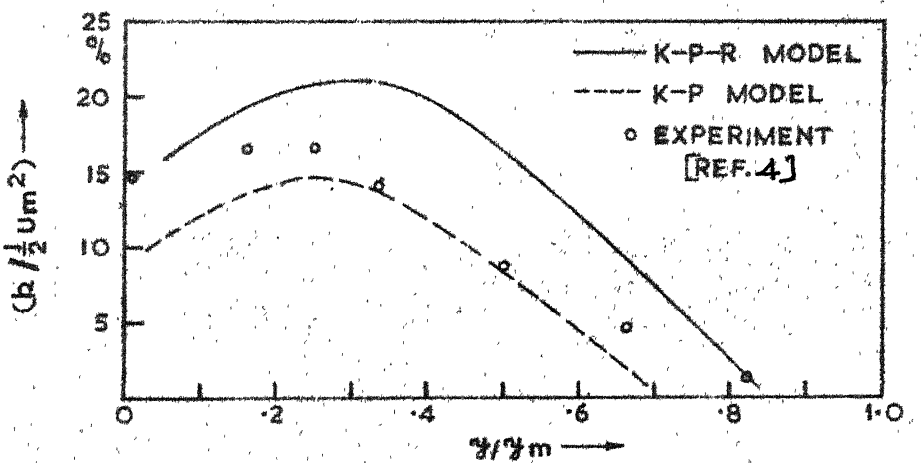

(c) VARIATION OF TURBULENT ENERGY 'k'

relation. Fig. (4-a) shows that the velocity profile obtained with this model is the same as that obtained by using the Prandtl mixing-length theory. Variation of k is shown in fig. (4-c) which is satisfactory having a peak value of 15% of $(\frac{1}{2}u_m^2)$.

With all the jet computations, the step length should be very properly adjusted. In the mixing zone we start with a smaller step length and gradually increase it to cover the mixing zone without doing wasteful computation. Then in the beginning of the transitional zone we have to again decrease the step length as in this region adjustments take place and big step lengths lead to oscillations.

c) Use of K-P-R model :-

The same set of constants that gave the results within the desired accuracy in the mixing layer, were used in the present case, and it was encouraging to find that we got satisfactory results in this case also.

We obtained the length of the potential core = 15, rate of growth $(y_{1/2}/x)$ = .13 which is higher than the experimental value reported in the beginning of this section. The centre line velocity is given by $(u_m/u_0) = 3{\cdot}25/\sqrt{x}$ and peak value of k = 21% of $(\frac{1}{2}u_m^2)$ which is satisfactory.

If we observe the velocity profile in fig. (4-a) we notice that velocity profile predicted with K-P-R model departs from the experimental points slightly more towards the low-velocity end. This is due to a higher value of $y_{1/2}$ which means that the predicted profile is 'fuller' than the experimental profile. A 'fuller' profile is explained by the accompanying sketch. If we use $y_{1/2}$ of the experimental profile we get the growth rate $y_{1/2}/x$ = .102 in place of .13. From this we conclude that a deeper study of the behaviour

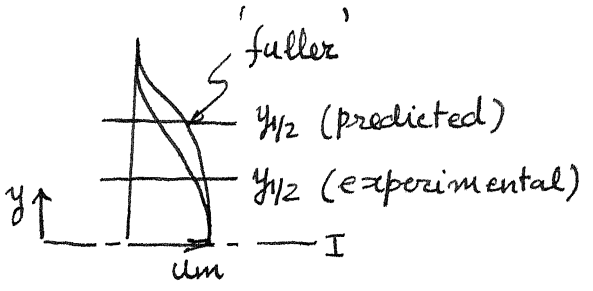

Sketch showing a
'fuller' profile.

of these constants is called for to get a better agreement with experiments in minute details. For the present we will be satisfied if the predicted gross quantities compare satisfactorily with experimental values. If in the present case we calculated the growth rate by y_E/x we get a value of about .27 as compared with an experimental value of .25.

The experimental data available for the turbulent quantities show a large variation and hence we shall not comment on the high level of turbulence (fig. 4c) predicted by the present model of turbulence.

(3.3) Round axisymmetric jet:-

The experimental results of round jet can be summarised as follows :

Growth rate $(y_{1/2}/x)$ = .09

$(u_m/u_0) = 6.5\, D_0/x$ (in some places 6.8 and 7 is also reported in place of 6.5) and so length of the potential core = about 6.5 dia meters. Peak value of k = about 25% of $(\frac{1}{2}u_m^2)$. This percentage is doubtful as Hinze (Ref. 5) mentions that Corrsin in his measurements has under estimated turbulence intensities.

a) Use of Prandtl mixing-length theory :-

The value of λ used was .105 with F = .1, computations were done for R_0 = 50. Length of the potential core obtained was about 720 i.e. 7.2 dia meters. The growth rate was $y_{1/2}/x$ =.081 and the centre line velocity is given by $(u_m/u_0) = 7.3\, D_0/x$ which compares well with experiments. The velocity profile obtained by our solution is shown in fig. (5-a) along with the experimental points. The variation of the centre-line velocity is shown in fig. (5-b). Scatter shown in this figure is due to the constant (.07) which has been used in abscisse. This constant is subject

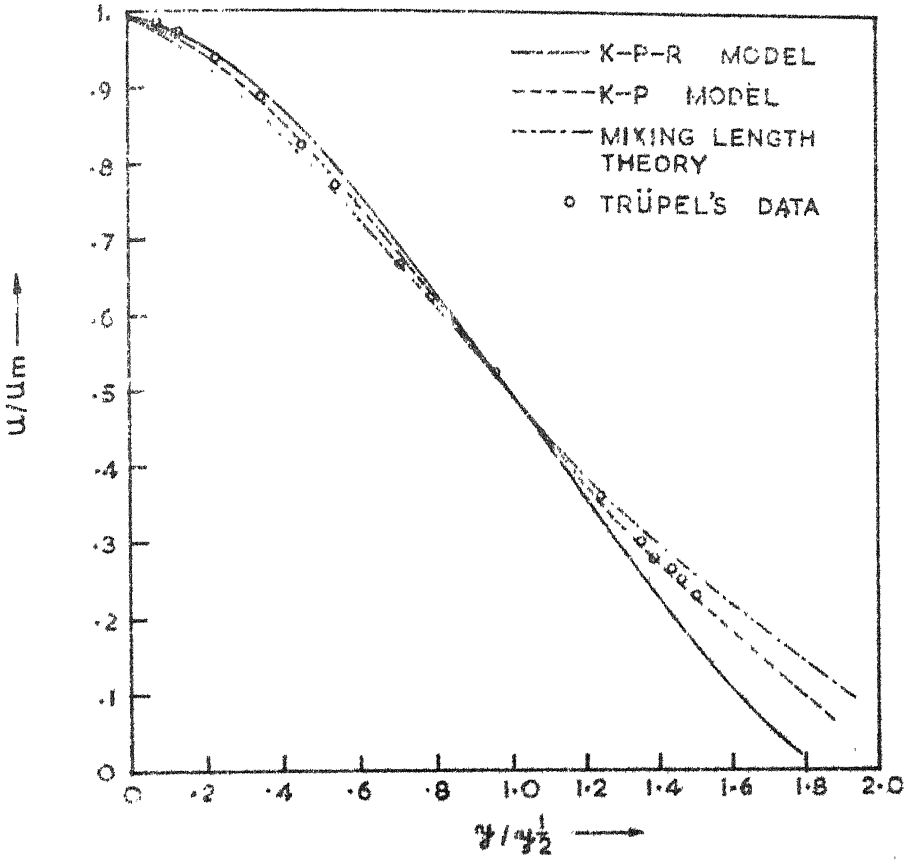

(a) DIMENSION LESS VELOCITY PROFILE

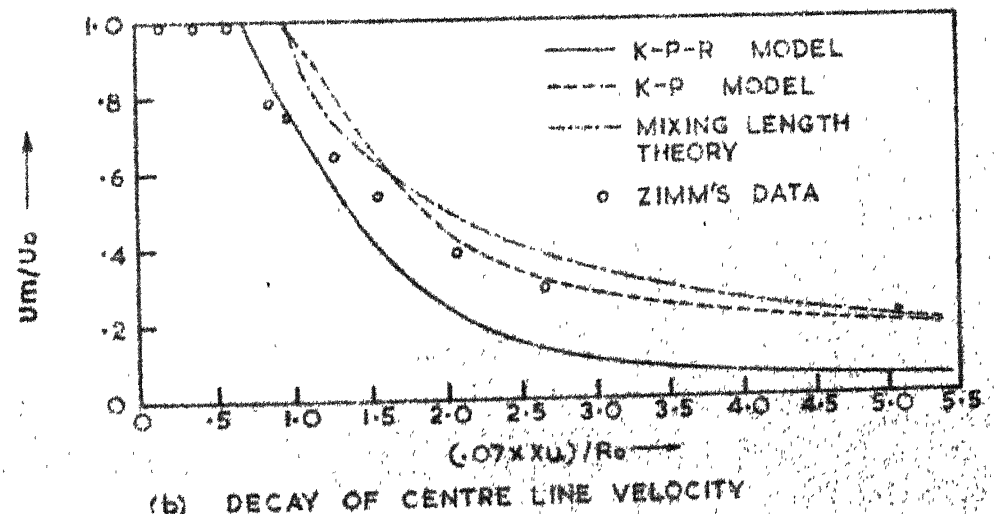

(b) DECAY OF CENTRE LINE VELOCITY

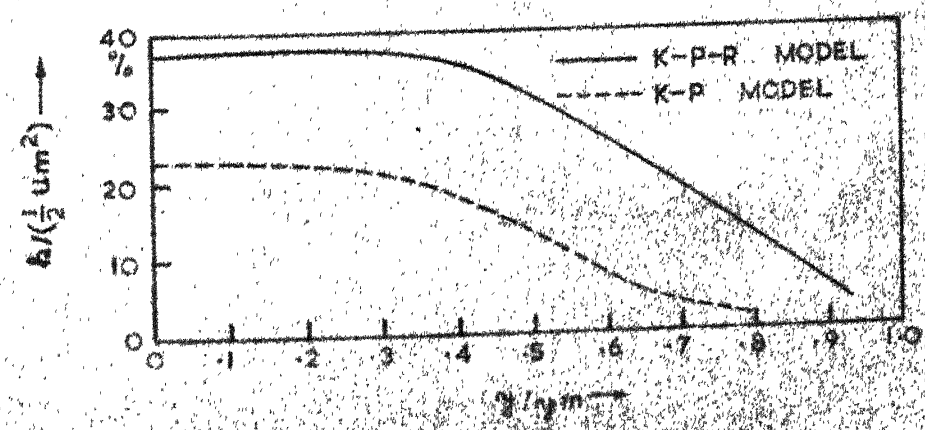

(C) VARIATION OF TURBULENT ENERGY 'k'

FIG.5 ROUND JET

to variation. We may not get good agreement with this constant. So we will give more importance to the relation that determines the decay of centre line velocity.

b) Use of K-P Model :-

Constants used were $C_D = .068$ and $\sigma_{k,eff} = 2.5$ with $\lambda_{K-P} = .037$ and $.058$ in mixing zone and region of main jet respectively. Results obtained were ;

Length of the potential core = 7.15 diameters.

Rate of growth $\cdot (y_{1/2}/x)$ = .092

and the centre-line velocity is given by $(u_m/u_o) = 6.25\, D_o/x$

It should be noted here that we should not make an estimate of the length of the potential core from the above relation for the centre-line velocity. We have used a different constant in the main jet region.

The peak value of k obtained is 23% of $(\frac{1}{2}u_m^2)$. In this model of turbulence peak value of k can be changed at one's choice by changing the constant C_D as it controls the dissipation of k. If 23% is not to be taken as satisfactory C_D can be decreased and higher intensity can be obtained; but in that computation other gross quantities might change. Therefore in view of a good agreement with the growth rate, the centre-line velocity and the dimensionless velocity profile [fig. (5-a)], this peak value of k intensity is satisfactory.

c) Use of K-P-R model :-

Constants used were again $C_D = .1$; $C_s = .4$; $C_{12} = .825$; $\sigma_{k,eff} = 2.5$; $\sigma_{kL,eff} = 2.5$ which are the same as used in case of mixing layer and the plane jet. We obtained using this set $y_{1/2}/x = .125$ $(u_m/u_o) = \frac{4.4\, D_o}{x}$ which shows a faster decay of the centre-line velocity.

The velocity profile as shown in fig. (5-a) is again fuller, which results in higher growth rate and so higher decay of the centre line velocity.

Peak value of k is about 38% of $(\frac{1}{2} u_m^2)$. In fig. (5-c) which shows the variation of k in the main jet experimental data is not shown as most of the data available either gives only 2 components of velocity fluctuations or corresponds to mixing zone.

(3.4) Fan jet:-

Not much experimental work has been done on fan jet. The following results are based on Tuve's data given in [Ref.1] . The growth rate (y_L/x) = .165 where y_L is the distance of the point where velocity is 10% of centre line velocity u_m from the centre line.

Centre line velocity decays according to

$$\frac{u_m}{u_o} = 3.8 \frac{\sqrt{r_o b_o}}{x}$$

where r_o = radius of the main pipe

and b_o = semi width of the slit.

There is no data available on turbulence characteristics of fan jet:

a) Use of Prandtl mixing-length theory:-

The value of λ used was .168 with F = .1. Use of this constant gave (y_L/x) = .167 and centre line velocity variation in the main jet exactly the same as given by the relation derived from the experimental results. However in the transition zone centre line velocity decay is not very well represented by this relation. In the transition zone decay is faster as is shown in fig. (6-b). Above value of λ gives a lower value of core length which shows that growth rate in mixing zone is higher. A lower value of λ in mixing zone would give the desired growth in that zone. As a consequence of higher rate of growth in the initial region, the centre-

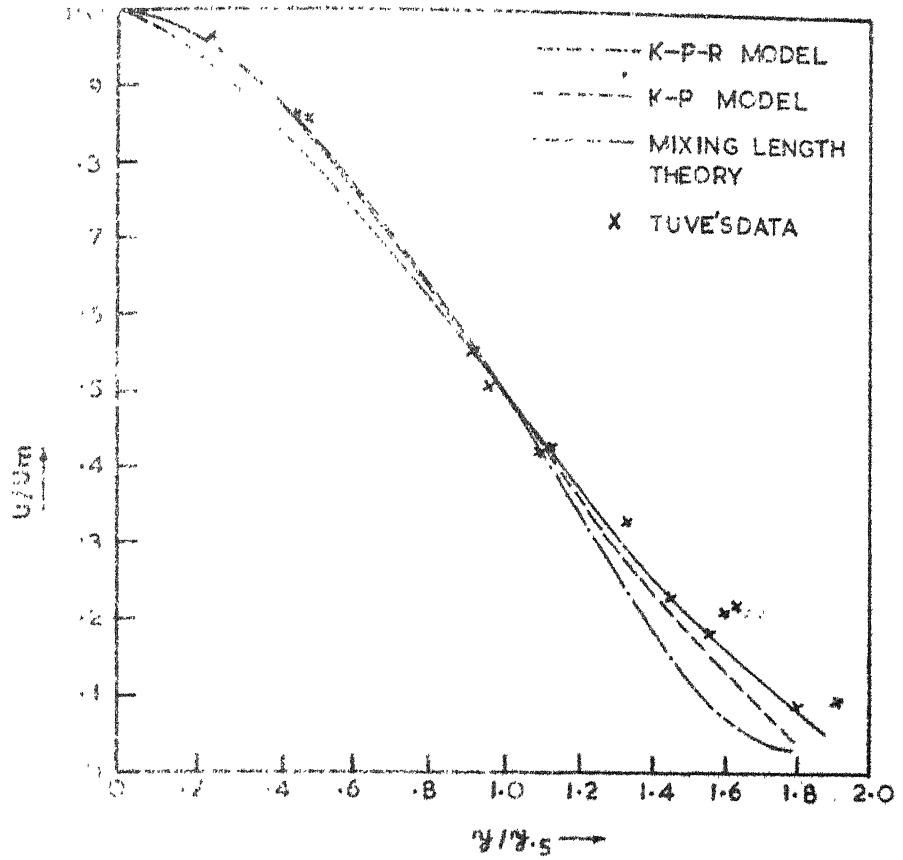

(a) DIMENSION LESS VELOCITY PROFILE

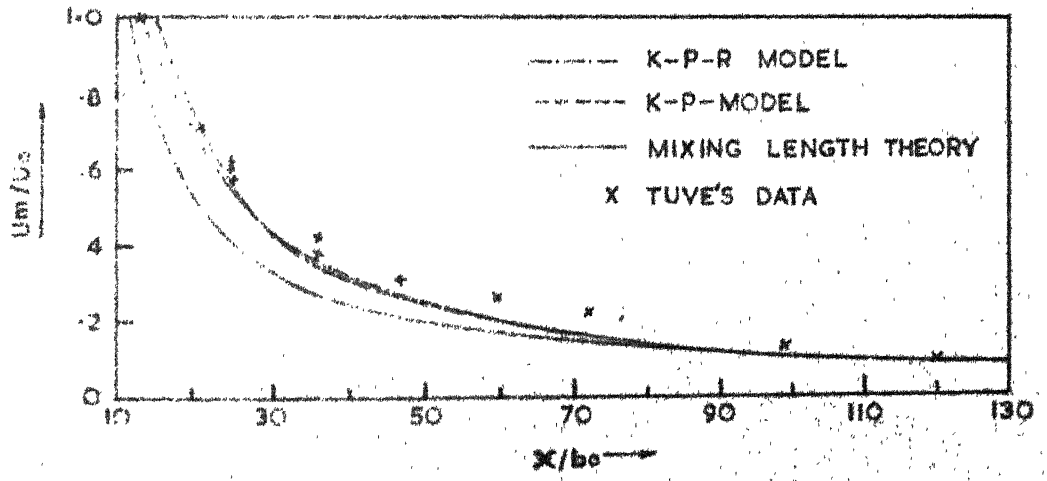

(b) DECAY OF CENTRE-LINE VELOCITY

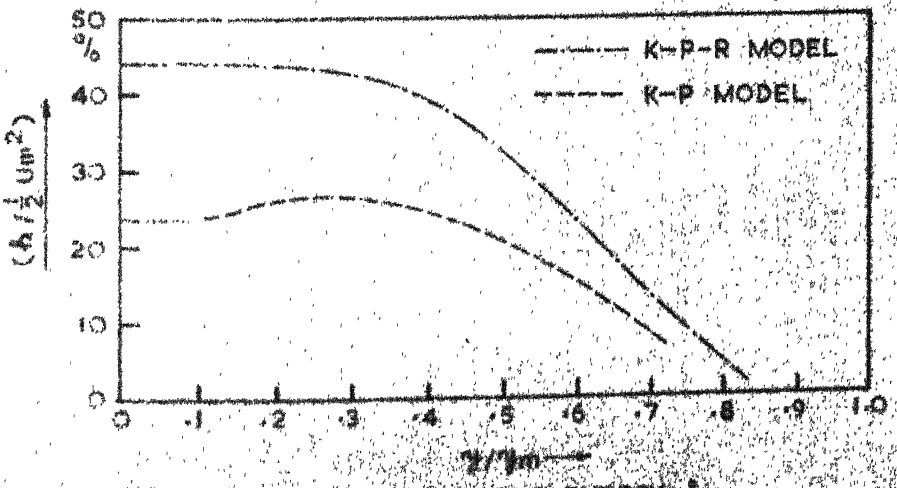

(c) VARIATION OF TURBULENT ENERGY &

FIG.6 FAN JET

line velocity decays at a faster rate in the transition zone and then gradually comes to the desired rate of decay.

b) Use of K-P model :-

Constants that gave satisfactory results were $\lambda_{K-P} = .084$ for mixing zone and $\lambda_{K-P} = .112$ for main jet with $F = .1$; $C_D = .14$ $\sigma_{k,eff} = 2.5$. These constants gave the following results:

Length of the potential core = 14 as against 12 in experiments.

Rate of growth $(y_{\frac{1}{2}}/x)$ = .171 which is satisfactory.

Centre line velocity follows the relation: $(u_m/u_0) = 13/x$ where as the experimental correlation is $\frac{u_m}{u_0} = \frac{12}{x}$ for $r_0 = 10$ and $b_0 = 1$. Peak value of k obtained was 27% of $(\frac{1}{2}u_m^2)$. The velocity profile as shown in fig. (6-a) compares satisfactorily with the experimental profile. To see the effect of C_D on the intensity of k, same computation was repeated with $C_D = .2$ keeping the other constants same. This resulted in decrease of k intensity and peak value came down to 17% of $(\frac{1}{2}u_m^2)$. However this profile is not shown in fig. (6-c).

c) Use of K-P-R model :-

Once again the previous set of constants was used and following results were obtained:

Core length = 14

Rate of growth $y_{\frac{1}{2}}/x$ = .185

Centre line velocity is given by $(u_m/u_0) = 13.2/x$

peak value of k = 44% of $(\frac{1}{2}u_m^2)$

Above results are satisfactory. Intensity of k is higher as predicted by this model as compared to that predicted by K-P model. Due to lack of experimental data none of the curves given in fig. (6-c) can be shown as particularly satisfactory. Velocity profile agrees

satisfactorily with experimental profile. Fig. (6-b) shows the curve for variation of the centre-line velocity with downstream distance. In this figure the predicted curve lies quite close to experimental points.

(3.5) General Remarks :-

The different sets of constants used in different cases have been collected in table-1. The Prandtl mixing-length theory and the K-P model need widely different constants for different flow cases to give the desired results. However the K-P-R model needs only one set of constants for all the four flow situations. This feature of the K-P-R model explains why the plane mixing layer, plane jet, round jet and the fan jet show similarities in growth rate etc. A closer observation of the length scale used in K-P-R model also explains why we need different empirical constants for different cases while using the Prandtl mixing-length theory. Fig. 7 shows the variation of L/y_L as obtained with the use of K-P-R model across the boundary layer for all the cases. As shown in the figure, the ratio L/y_L remains nearly uniform at all x's , in each case. This is consistent with the practice used in the Prandtl mixing-length theory that the length scale is made proportional to some characteristic thickness of boundary layer. Secondly we notice in Fig. 7 that L/y_L has a different value for each case. L/y_L corresponds to λ used in mixing length theory and hence different levels of L/y_L lines in fig. 7 explain the different values of λ to be used with the mixing-length theory. L/y_L level for fan jet is highest which is consistent with the value of λ used in fan jet. With this we fulfil the aim set up in the introduction of the thesis.

The next section of this chapter contains an example of

TABLE - 1

Flow situation	Prandtl's mixing length theory.	Kolmogorov - Prandtl model.	Kolmogorov-Prandtl-Ratta model
Plane mixing layer.	λ = .117 (F= .1)	λ_{k-p} = .066 (F = .1) $\sigma_{R,eff}$ = 2.5 C_D = .1	C_D = .1; β_s = .4; β_{12} =.825 $\sigma_{R,eff}$ = 2.5 ; $\sigma_{RL,eff}$ = 2.5
Plane jet.	λ = .141 (F= .2)	λ_{k-p} = .1 for mixing zone (F = .2) λ_{k-p} =.08 for main jet. $\sigma_{R,eff}$ =2.5; C_D = .1	C_D = .1; β_s = .4; β_{12} =.825 $\sigma_{R,eff}$ = 2.5 ; $\sigma_{RL,eff}$ = 2.5
Round jet.	λ = .105 (F= .1)	λ_{k-p} =.037 for mixing zone (F = .1) λ_{k-p} =.058 for main jet. $\sigma_{R,eff}$ =2.5; C_D =.068	C_D = .1; β_s =.4; β_{12} =.825 $\sigma_{R,eff}$ = 2.5; $\sigma_{RL,eff}$ =2.5
Fan jet	λ = .168 (F = .1)	λ_{k-p} =.084 for mixing zone (F=.1) λ_{k-p} =.112 for main jet $\sigma_{R,eff}$ = 2.5 C_D = .14	C_D = .1; β_s =.4; β_{12} =.825 $\sigma_{R,eff}$ = 2.5 ; $\sigma_{RL,eff}$ = 2.5

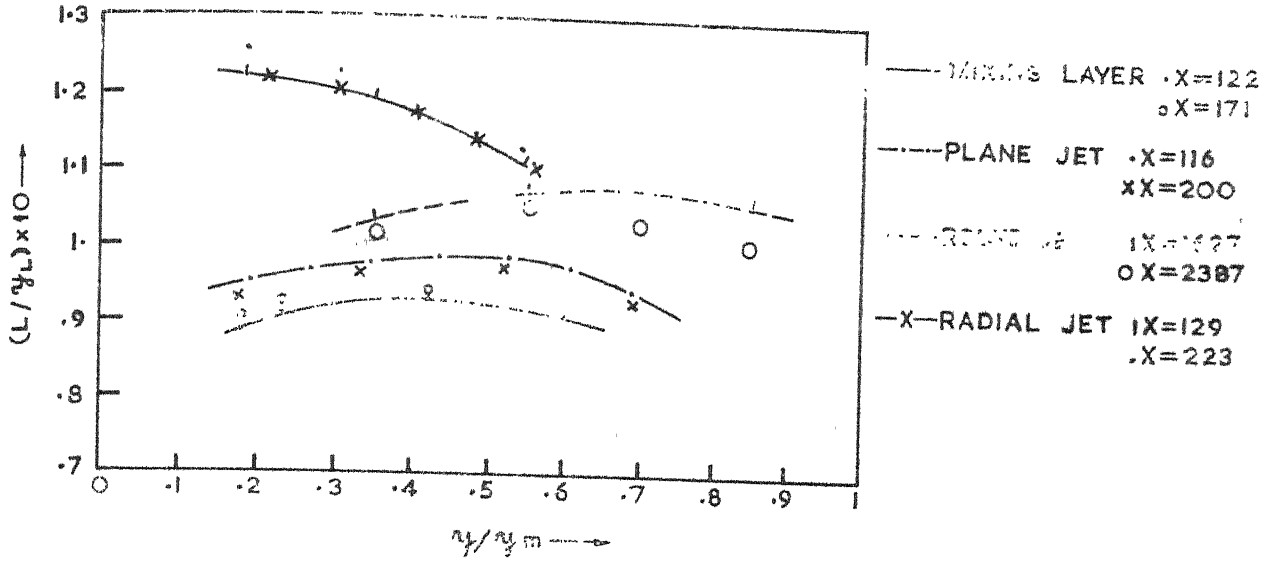

FIG. 7

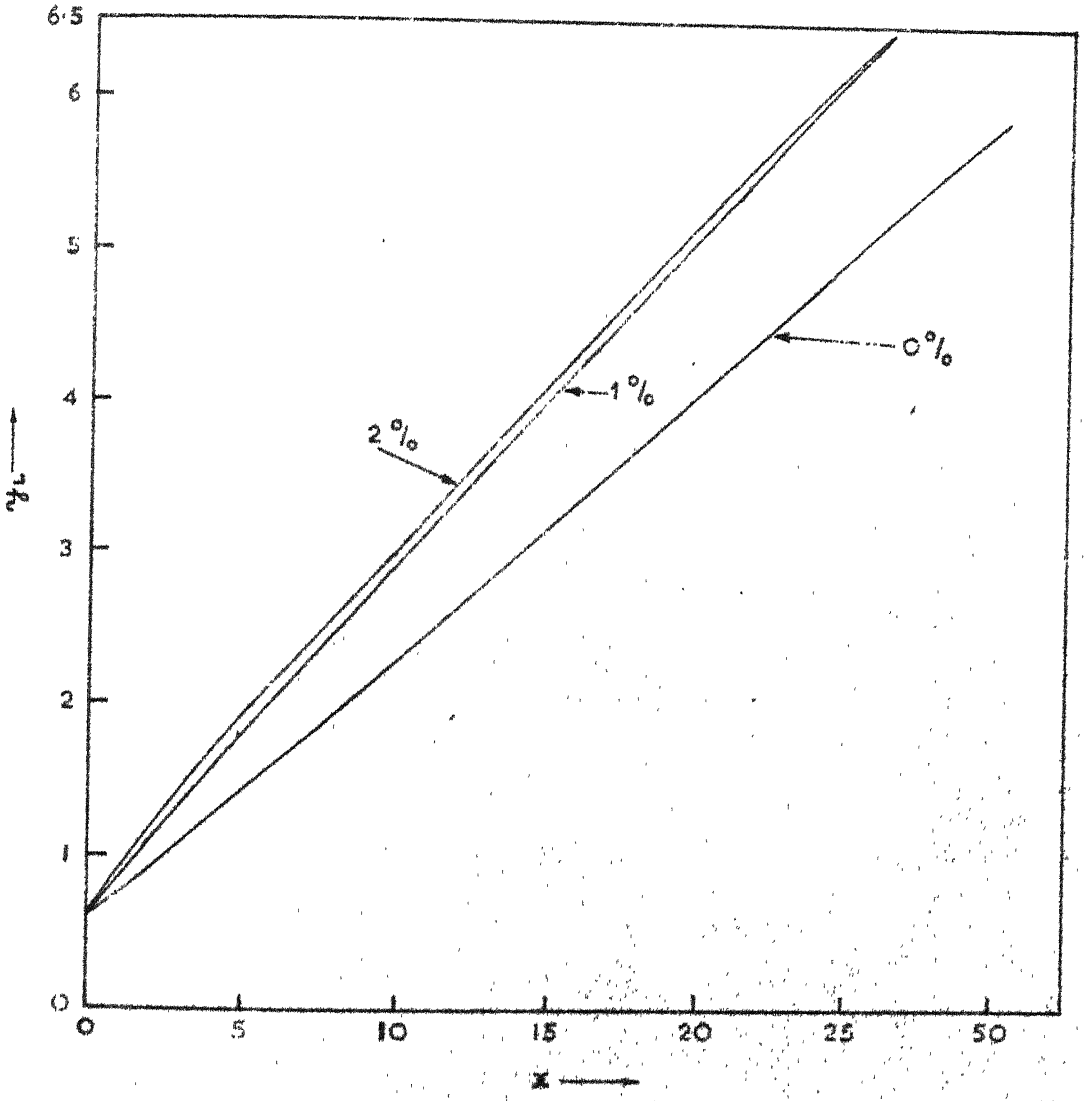

FIG.8 EFFECT OF FREE-STREAM TURBULENCE ON BOUNDARY LAYER GROWTH

the extension of present work.

(3.6) Effect of free-stream turbulence :-

We have dealt with the special case of stagnant surroundings. In quite a few practical applications jets are injected in the fluid streams that are flowing in the direction of the jet and in some cases in the opposite direction also. The effect of moving surroundings on the growth rate and other features of the flows remains to be investigated. It is expected that the set of constants found out in the present thesis will work in case of moving surroundings also.

In case of the mixing layer we assumed that the free stream of uniform velocity is free from turbulence. In high velocity streams some turbulence intensities are usually present. So the effect of free-stream turbulence ought to be studied. Some computations were done with presence of free-stream turbulence towards the end of the present work. Results obtained are shown in fig.8. Because of the turbulence at the external boundary, rate of growth increases in the beginning and then falls down gradually to the value obtained in absence of free-stream turbulence. Only cases of low free-stream turbulence are reported in the fig. 8. The curve for a free-stream turbulence equal to 2% of $(\frac{1}{2} u_e^2)$ shows slightly higher growth rate than 1% free-stream turbulence in the initial region and then the two curves meet each other after which growth rate decays at the same rate. If we apply the conservation equation for k in the free stream we get:

$$dk/dx = - C_D S_s \, k^{3/2}/L \qquad (36)$$

Eq. (36) shows that k decays in free stream and rate of decay is faster at higher values of k . This explains why the two growth rates corresponding to different initial free-stream turbulences become equal after some distance.

The same set of empirical constants was used in these computations. Such effects are yet to be seen for other flows.

R_E_F_E_R_E_N_C_E_S

1. ABRAMOVICH, G.N. (1963) The theory of turbulent jets. M.I.T. Press.
2. CSANADY, G.T. (1963) J. Fluid Mech., 15, pp. 545.
3. EMMONS, H.W. (1954) Shear flow turbulence. Proc. of 2nd U.S. Nat Congress of Applied Mechanics.
4. HESKESTAD, GUNNAR (1965) Hot wire measurements in plane turbulent jets/J. Applied Mechanics, Trans.ASME, Series E, Vol. 32, pp. 721.
5. HINZE, J.O. (1959) Turbulence. McGraw-Hill Book Company, INC.
6. PATANKAR, S.V. and SPALDING, D.B. (1967) Heat and Mass transfer in Boundary Layers, Morgan-Grampian: London.
7. Progress in Aeronautical Sciences, Vol. 2, Edited by Ferri, Küchemann and Sterne.
8. ROTTA, J. (1951) Statistische theorie nichthomogener Turbulenz. Z. für Physik, Vol. 131, pp. 51-77.
9. SHIN-I PAI (1954) Fluid dynamics of jets. D. Van Nostrand Company, INC.
10. SPALDING, D.B. (1967) The calculation of the length scale of turbulence in some turbulent boundary layers remote from walls, Imperial College, Mechanical Engineering Dept., report TWF/TN/31
11. SPALDING, D.B. (1967) Monograph on Turbulent Boundary Layers- Chapter 1, Imperial College, Mech. Engg. Dept., Report TWF/TN/24 and Chapter 3, TWF/TN/35.

NOMENCLATURE.

Symbol.	Meaning.
A, B, C	coefficients in the difference equation.
a, b, c, d	defined in eq. (20).
J	turbulent diffusional flux.
k	kinetic energy of fluctuations per unit mass.
L	length scale in K-P model and K-P-R model.
ℓ	Prandtl's mixing length.
$\dot{m}''$	mass transfer rate a cross a boundary.
N	number of strips a cross a layer.
r	distance from axis of symmetry.
$\bar{u}_1, u$	velocity in the longitudinal direction.
$\bar{u}^*$	desired velocity defined by eq.(28)
ω	nondimensionalised stream function. $(\psi - \psi_I)/(\psi_E - \psi_I)$
y_L	characteristic thickness of the boundary layer.
ρ	density of the fluid.
ν	kinematic viscosity of the fluid.
μ	laminar viscosity of the fluid.
μ_{eff}	effective viscosity.
σ_{eff}	effective Prandtl number.
ϕ	a general dependant variable.
$\bar{\Phi}$	source term.
ψ	stream function

Subscripts:

d, D	the downstream point on a portion of the grid.
E	the external boundary of the layer .
I	the internal boundary of the layer.
k	pertaining to kinetic energy of fluctuations.
kL	pertaining to the variable (kL)
U	the upstream point on a portion of the grid.
m	refers to maximum value.
o	condition at the jet efflux.

A P P E N D I X

Conservation equations for (kL) and L as given by Rotta (1951) :-

Rotta (Ref. 8) in the following derivation has used the statistical approach to turbulence introduced by G.I. Taylor in 1935. According to this approach the turbulent energy k is distributed in a very large number of turbulence - elements or eddies of different sizes. The length scale of turbulence is thought of as the mean dia meter of these eddies. Temporal and spatial changes in this length scale have an immediate influence on the different processes in turbulence. The structure of turbulence is described by the statistical correlation between the fluctuating quantities. This description is given in theory by means of some spectral functions. These spectral functions are Fourier transforms of the correlation functions. A spectral function represents the contribution to the corresponding correlation function by the wave numbers between m and $m+dm$, wave number m being the reciprocal of the length scale.

The total turbulent energy per unit mass at a point is defined in terms of correlation function and spectral function as follows :

$$k(r_c,t) = \sum_{i=1}^{3} \frac{\overline{u_i^2}}{2} = \int_0^\infty F(m,r_c,t)\, dm \qquad \text{——————} \quad (a\text{-}1)$$

where r_c is the position vector of the point. In eq. (a-1) the spectral function $F(m,r_c,t)$ represents contribution to k by the wave number between m & $m+dm$. The characteristic length scale of turbulence L is defined by the relation

$$L(r_c,t) = \frac{3\pi}{8k(r_c,t)} \int_0^\infty F(m,r_c,t)\, \frac{dm}{m} \qquad \text{——————} \quad (a\text{-}2)$$

where the factor $\frac{3\pi}{8}$ comes from considerations of isotropic turbulence.

Starting from the general Navier - Stokes equations of motion Rotta reaches at the following equation for the spectral function F, after some complicated algebra :

$$\frac{\partial F(m,r_c,t)}{\partial t} + \sum_{n=1}^{3} \bar{u}_n \frac{\partial F(m,r_c,t)}{\partial x_n} + \sum_{i=1}^{3}\sum_{n=1}^{3} F_{in}(m,r_c,t) \frac{\partial \bar{u}_i}{\partial x_n} + \sum_{n=1}^{3} \frac{\partial F_a^{\,w}(m,r_c,t)}{\partial x_n}$$

$$- \nu \Delta F(m,r_c,t) + F_s(m,r_c,t) = 0 \qquad \text{——— (a-3)}$$

The first two terms of eq. (a-3) represent the total change in the fluctuating kinetic energy spectrum. The third term represents the work done by the Reynold stresses. $F_{in}(m,r_c,t)$ is the contribution to Reynold stresses by the wave numbers between m and $m+dm$. The fourth term represents the effect of turbulent diffusion of k in direction n on the spectrum of k . $F_a^{\,w}$ is the spectral function for turbulent diffusion of k in n direction. The term containing ν in eq. (a-3) shows the effect of viscous diffusion of k and is small for free turbulent flows. The last term is the spectral function for dissipation of k .

Multiplying eq. (a-3) by $\frac{3\pi}{8m}$ and integrating each term with respect to m from 0 to ∞ , the following equation for (kL) is obtained after making use of eq. (a-2):

$$\frac{\partial}{\partial t}(kL) + \sum_{n=1}^{3} \bar{u}_n \frac{\partial}{\partial x_n}(kL) + \sum_{n=1}^{3}\sum_{i=1}^{3} \frac{3\pi}{8} \int_0^\infty F_{in} \frac{dm}{m} \frac{\partial \bar{u}_i}{\partial x_n} + \sum_{n=1}^{3} \frac{\partial}{\partial x_n}\left(\frac{3\pi}{8}\int_0^\infty F_a^{\,w} \frac{dm}{m}\right)$$

$$+ \frac{3\pi}{8}\int_0^\infty F_s \frac{dm}{m} = 0 \qquad \text{——— (a-4)}$$

Now eq. (a-3) is multiplied by L and integrated with respect to m from 0 to ∞ . The resulting equation when subtracted from eq.(a-4) gives the differential equation for the length scale. The equation for L has the following form:

$$k\left(\frac{\partial L}{\partial t} + \sum_{n=1}^{3} \bar{u}_n \frac{\partial L}{\partial x_n}\right) + \sum_{i=1}^{3}\sum_{n=1}^{3} \int_0^\infty F_{in}\left(\frac{3\pi}{8m} - L\right) dm \frac{\partial \bar{u}_i}{\partial x_n} + \sum_{n=1}^{3} \frac{\partial}{\partial x_n}\left(\frac{3\pi}{8}\int_0^\infty F_a^{\,w} \frac{dm}{m}\right)$$

$$-L \sum_{n=1}^{3} \int_0^\infty F_a^{\,w}\, dm + \int_0^\infty F_s\left(\frac{3\pi}{8m} - L\right) dm = 0 \qquad \text{——— (a-5)}$$

Like all other conservation equations, the conservation equation for L given by eq. (a-5) relates the total change of L with the effect of energy generation, diffusion and dissipation on L.

We come back to eq. (a-4) and make the following postulates so that the equation becomes suitable for application:

(I) It is assumed that a spectral function can be represented in terms of a dimensionless function as shown by the following relations:

$$\left.\begin{aligned} F_{in} &= \overline{u_i' u_n'}\, L\, f_{in}(\psi) \\ F_s &= D' L\, f_s(\psi) \end{aligned}\right\} \qquad \text{——— (a-6)}$$

where $\psi = mL$, $\overline{u_i' u_n'}$ stand for Reynold stresses, and D' is the net dissipation of k per unitmass. Using eq. (a-1) with this postulate it can be seen that the dimensionless functions f satisfy the equation

$$\int_0^\infty f(\psi)\, d\psi = 1 \qquad \text{——— (a-7)}$$

(II) It is assumed that the integral $\int_0^\infty f(\psi)\, \frac{d\psi}{\psi}$ is a constant independent of space, time and other factors in turbulence. This means that we can write

$$\frac{3\pi}{8} \int_0^\infty f(\psi)\, \frac{d\psi}{\psi} = \beta \ (\text{const.}) \qquad \text{——— (a-8)}$$

We will have two constants β_{in} and β_s corresponding to the dimensionless functions f_{in} and f_s respectively.

(III) It is assumed that the spectral function for diffusion F_a^w can be expressed by an exchange law analogous to the exchange law that is used for the diffusional flux. With this postulate we can write

$$F_a^w = -\epsilon_n \frac{\partial F(m, r_c, t)}{\partial x_n} \qquad \text{——— (a-9)}$$

where ϵ_n is the exchange coefficient and F is the energy spectral function given by eq. (a-1). It is further assumed that ϵ_n depends upon the wave number m and can be represented by a dimensionless

function $\Phi(\chi)$ as follows:

where ε_n is same as $\epsilon_n(m) = \varepsilon_n \Phi(\chi)$ ——————(a-10)

$\therefore \quad F_a^w = -\varepsilon_n \Phi(\chi) \frac{\partial F}{\partial x_n}$

using postulate (I) for F we have

$F_a^w = -\varepsilon_n \Phi(\chi) \frac{\partial}{\partial x_n}(kLf)$

or $F_a^n \frac{dm}{m} = -\varepsilon_n \Phi(\chi) f(\chi) \frac{\partial}{\partial x_n}(kL)$ ——————(a-11)

Integrating eq. (a-11) with respect to and using postulate (II) we get

$$\int_0^\infty F_a^w \frac{dm}{m} = -\varepsilon_n \rho_a \frac{\partial}{\partial x_n}(kL) \qquad \text{——————(a-12)}$$

where ρ_a° is a constant.

Using the above postulates eq. (a-4) can be put in the following form for steady, two dimensional boundary layers:

$$\rho \bar{u}_1 \frac{\partial}{\partial x_1}(kL) + \rho \bar{u}_2 \frac{\partial(kL)}{\partial x_2} - \mu_{eff} L \rho_{12} \left(\frac{\partial \bar{u}_1}{\partial x_2}\right)^2 - \frac{\partial}{\partial x_2}\left(\frac{\mu_{eff}}{\sigma_{k,eff}} \rho_a \frac{\partial(kL)}{\partial x_2}\right)$$

$$+ DL \rho_s = 0 \qquad \text{——————(a-13)}$$

eq. (a-13) on transformation to axisymmetric coordinate system reduces to the eq. (15) given in section (1.33) of Chapter 1.

Not much is known about the constants ρ_{12}, ρ_s and ρ_a. Based on the theory of homogeneous and isotropic turbulence and experiments on turbulent flow of air behind a mesh carried out by Batchelor and Townsend (1948), Rotta suggests a value of .8 for ρ_s. From the study of fully developed turbulent flow in channels and pipes of uniform cross section Rotta concludes that ρ_a should be equal to ρ_s and ρ_{12} should be more than ρ_s by 10% ($\rho_{12} = 0.88$). These values of constants may not be used in our prediction procedure, however with this estimate we get an idea of the order of magnitude of these constants.